Functional CT imaging for identification of the spatial determinants of small-airways disease in adults with asthma

Alex J. Bell, MMath,[a] Brody H. Foy, BMath,[b] Matthew Richardson, PhD,[a] Amisha Singapuri, BSc,[a] Evgeny Mirkes, PhD,[c] Maarten van den Berge, PhD,[d] David Kay, PhD,[b] Chris Brightling, FRCP, PhD,[a] Alexander N. Gorban, PhD,[c] Craig J. Galbán, PhD,[e] and Salman Siddiqui, FRCP, PhD[a]

Leicester and Oxford, United Kingdom, Groningen, The Netherlands, and Ann Arbor, Mich

Background: Asthma is a disease characterized by ventilation heterogeneity (VH). A number of studies have demonstrated that VH markers derived by using impulse oscillometry (IOS) or multiple-breath washout (MBW) are associated with key asthmatic patient–related outcome measures and airways hyperresponsiveness. However, the topographical mechanisms of VH in the lung remain poorly understood.

Objectives: We hypothesized that specific regionalization of topographical small-airway disease would best account for IOS- and MBW-measured indices in patients.

Methods: We evaluated the results of paired expiratory/inspiratory computed tomography in a cohort of asthmatic (n = 41) and healthy (n = 11) volunteers to understand the determinants of clinical VH indices commonly reported by using IOS and MBW. Parametric response mapping (PRM) was used to calculate the functional small-airways disease marker PRM^{fSAD} and Hounsfield unit (HU)–based density changes from total lung capacity to functional residual capacity (ΔHU); gradients of ΔHU in gravitationally perpendicular (parallel) inferior-superior (anterior-posterior) axes were quantified.

Results: The ΔHU gradient in the inferior-superior axis provided the highest level of discrimination of both acinar VH (measured by using phase 3 slope analysis of multiple-breath washout data) and resistance at 5 Hz minus resistance at 20 Hz measured by using impulse oscillometry (R5-R20) values. Patients with a high inferior-superior ΔHU gradient demonstrated evidence of reduced specific ventilation in the lower lobes of the lungs and high levels of PRM^{fSAD}. A computational small-airway tree model confirmed that constriction of gravitationally dependent, lower-zone, small-airway branches would promote the largest increases in R5-R20 values. Ventilation gradients correlated with asthma control and quality of life but not with exacerbation frequency.

Conclusions: Lower lobe–predominant small-airways disease is a major driver of clinically measured VH in adults with asthma. (J Allergy Clin Immunol 2019;144:83-93.)

Key words: *Asthma, computed tomography, parametric response mapping, imaging, visualization, small-airways physiology, biomarker*

Asthma is characterized by spatial heterogeneity in disease and consequent heterogeneity in airways function and lung ventilation.[1,2] Ventilation heterogeneity (VH) can be captured by using imaging approaches that can quantify and regionalize lung ventilation, such as hyperpolarized helium-3/xenon-129 magnetic resonance imaging (MRI), oxygen-enhanced magnetic resonance, and single-photon emission computed tomography (CT).[3-7] Additionally, VH can be measured clinically in patients by using physiologic tidal breathing techniques that measure heterogeneities in lung ventilation (captured by using multiple-breath washout [MBW])[8,9] and mechanical behavior (captured by using impulse oscillometry [IOS]).[10] International guidelines for quality control and assurance of tidal breathing markers of VH derived from IOS and MBW have been proposed,[11,12] supporting their potential role as tools to study early airways disease.

We have previously identified that 2 specific markers of VH, resistance at 5 Hz minus resistance at 20 Hz measured by using impulse oscillometry (R5-R20) and acinar VH (S_{acin}; measured by using phase 3 slope analysis of multiple-breath washout data), derived from IOS and MBW, respectively, are associated with impaired asthma control, quality of life, and

From [a]the NIHR Respiratory Biomedical Research Centre (BRC), Department of Respiratory Sciences, and [c]the Department of Mathematics, University of Leicester; [b]Computational Biology, Department of Computer Science, University of Oxford; [d]the Department of Pulmonology, University Medical Centre Groningen; and [e]the Department of Radiology, University of Michigan, Ann Arbor.

Supported by the Sir Jules Thorn trust, "Systems medicine: novel mathematical approaches to personalized care in asthma patients," through a clinical senior lecturer award (Professor Siddiqui). Additional funding was received for the original computed tomographic scan and physiologic analyses from Roche Pharmaceuticals (C.B. and S.S.) and the European Union Airways Disease Predicting Outcomes in Patient Specific Computational Models (AirPROM-FP7) consortium. This article was also supported by the National Institute for Health Research (NIHR) Leicester Respiratory Biomedical Research Centre (BRC). The views expressed are those of the author(s) and not necessarily those of the National Health Service, the NIHR, or the Department of Health.

Disclosure of potential conflict of interest: B. H. Foy reports grants from the Rhodes Trust and nonfinancial support from and AirPROM-FP7 grant during the conduct of the study. C. Brightling reports grants from the NIHR Biomedical Research Centre and EU FP7 during the conduct of the study; grants and personal fees from GlaxoSmithKline, AstraZeneca, MedImmune, Boehringer Ingelheim, Roche/Genentech, Novartis, Chiesi, and Mologic; and personal fees from PreP, 4DPharma, TEVA, Gilead, and Glenmark outside the submitted work. S. Siddiqui reports grants from the NIHR Biomedical Research Centre, grants from Sir Jules Thorne Trust, a clinical senior lecturer award (Professor Siddiqui), and grants from EU-FP7 AirPROM during the conduct of the study; other support from AstraZeneca, GlaxoSmithKline, Owlstone Medical, Mundipharma, and Boehringer Ingelheim; and personal fees from the European Respiratory Society outside the submitted work. The rest of the authors declare that they have no relevant conflicts of interest.

Received for publication April 12, 2018; revised January 9, 2019; accepted for publication January 14, 2019.

Available online January 22, 2019.

Corresponding author: Salman Siddiqui, MRCP, PhD, NIHR Biomedical Research Centre (Respiratory Theme), Respiratory BRU Building Glenfield Hospital, Groby Rd, Leicester LE3 9QP, United Kingdom. E-mail: ss338@leicester.ac.uk.

0091-6749/$36.00

https://doi.org/10.1016/j.jaci.2019.01.014

Abbreviations used

ATS: American Thoracic Society
ERS: European Respiratory Society
FRC: Functional residual capacity
fSAD: Functional small-airways disease
FVC: Forced vital capacity
GINA: Global Initiative for Asthma
HU: Hounsfield units
IOS: Impulse oscillometry
LDA: Linear discriminant analysis
MBW: Multiple-breath washout
MRI: Magnetic resonance imaging
PRM: Parametric response mapping
R5-R20: Resistance at 5 Hz minus resistance at 20 Hz measured by using impulse oscillometry
SAA: Stratified axial analysis
S_{acin}: Acinar ventilation heterogeneity (measured using phase 3 slope analysis of multiple-breath washout data)
SF_6: Sulfur hexafluoride
TLC: Total lung capacity
VH: Ventilation heterogeneity

exacerbations.[9,13] These observations have been replicated by other groups in parallel studies of adult asthma.[14,15] Additionally, using computational small-airway models and diffusion MRI, we have previously demonstrated that IOS-derived R5-R20 and MBW-derived S_{acin} values are anatomically grounded measures of small and acinar airway anatomic disease, respectively, in adult asthmatic patients.[9]

Heterogeneity of ventilation within the lungs is likely to be influenced by both gravitational effects and airway branching, as well as other factors that affect regional lung compliance.[16] However, little is known about the spatial lung determinants of clinical measurements of VH derived by using MBW and IOS. This is important because imaging tools are costly and difficult to implement in clinical trials and standardize across centers; physiologic tools, if appropriately validated, could serve as simple surrogates of disease heterogeneity captured by using sensitive imaging techniques.

CT of the lungs has been exploited widely to study lung structure and function relationships in asthmatic patients.[17,18] More recently, image registration applied to inspiratory and expiratory CT imaging has been used to derive indices of functional small-airways disease (fSAD).[19-22] One specific and widely deployed approach is parametric response mapping (PRM).[20-22] The PRM approach offers the potential to characterize spatial deformation of a voxel between different acquired CT lung volumes, such as functional residual capacity (FRC) and total lung capacity (TLC), over the entire lung and hence the potential to identify spatial mechanisms of commonly measured MBW and IOS VH markers.

The purpose of this study was to use a range of global and regional airway density change (from FRC to TLC) imaging biomarkers to understand how spatial variations in VH can contribute to widely reported clinical measurements of VH and small-airways disease captured by IOS and MBW in adult asthmatic patients. Specifically, we hypothesized that abnormal regional variations in Hounsfield units (HU [ΔHU]) would be a major contributor to abnormal IOS- and MBW-derived physiologic indices of VH in the small airways and sought to test this hypothesis using a functional CT imaging and computational simulation study.

METHODS

Subjects

The total population for this study consisted of 52 subjects, 41 adult asthmatic patients and 11 healthy control subjects. Asthmatic patients were recruited from Glenfield Hospital, Leicester, United Kingdom.

Asthma was defined by a clinician's diagnosis with 1 or more of the following objective criteria: (1) bronchodilator reversibility of FEV_1 to 400 μg of inhaled salbutamol of 12% and 200 mL or greater (17/41 asthmatic patients), (2) methacholine PC_{20} of 16 mg/mL or less (11/41 asthmatic patients), or (3) peak flow variation of 20% or greater over a 2-week period (13/41 asthmatic patients).

Asthma severity was classified according to current Global Initiative for Asthma (GINA) treatment steps.[23] Patients with severe asthma within the cohort had similar lung function (postbronchodilator FEV_1/forced vital capacity [FVC] ratio) to previously reported severe asthma cohorts in Leicester, United Kingdom,[24] but greater average postbronchodilator FEV_1 percent predicted values.

Age-matched healthy volunteers were recruited through local advertising and staff, with normal airway physiology and no features of respiratory disease. All asthmatic patients had been free from exacerbations for at least 6 weeks before study entry.

All subjects (both asthmatic patients and healthy volunteers) were noncurrent smokers; however, because of the known association of smoking and small-airways disease, pack year smoking exposure was not an exclusion criterion. Only 3 of 41 patients with asthma had a smoking history of more than 15 pack years.

Ethical approval

The study protocol was approved by the National Research Ethics Committee–East Midlands Leicester (approval no. 08/H0406/189), and all subjects provided written informed consent.

Visits

Clinical and physiologic assessment was performed in the following sequence and over 1 to 2 study visits no more than 1 week apart. Asthma control was characterized by using the modified 6-item Juniper Asthma Control Questionnaire,[25] and asthma quality of life was characterized by using the standard 32-question Juniper Asthma Quality of Life Questionnaire.[26] Exacerbations were defined according to American Thoracic Society (ATS)/European Respiratory Society (ERS) consensus criteria.[27] A moderate-to-severe exacerbation is defined as 1 or more of the following: (1) worsening of asthma that requires use of systemic steroids or an increase in systemic steroid use (for patients already receiving maintenance oral steroids) for 3 or more days or (2) an admission to the hospital or an emergency department requiring systemic steroids.

Lung function measurements

All lung function tests were performed after administration of 400 μg of inhaled salbutamol. Spirometry was performed according to ATS/ERS standards.[28]

IOS was performed in triplicate, as previously reported, and in accordance with international guidelines.[11,12] MBW was performed according to current guidelines[12] by using the sulfur hexafluoride (SF_6) wash-in method, as previously described.[13] SF_6 was chosen as the inert tracer gas because of its heavy molar mass and based on previous simulation data from Dutrieue et al,[29] suggesting that phase III slope sensitivity to SF_6 is maximal at the level of the alveolar duct. The phase III slope indices S_{cond} (conductive zone VH) and S_{acin} (acinar zone VH) were calculated by using custom software written with TestPoint (Measurement Computing, Norton, Mass), as previously described.[9,13]

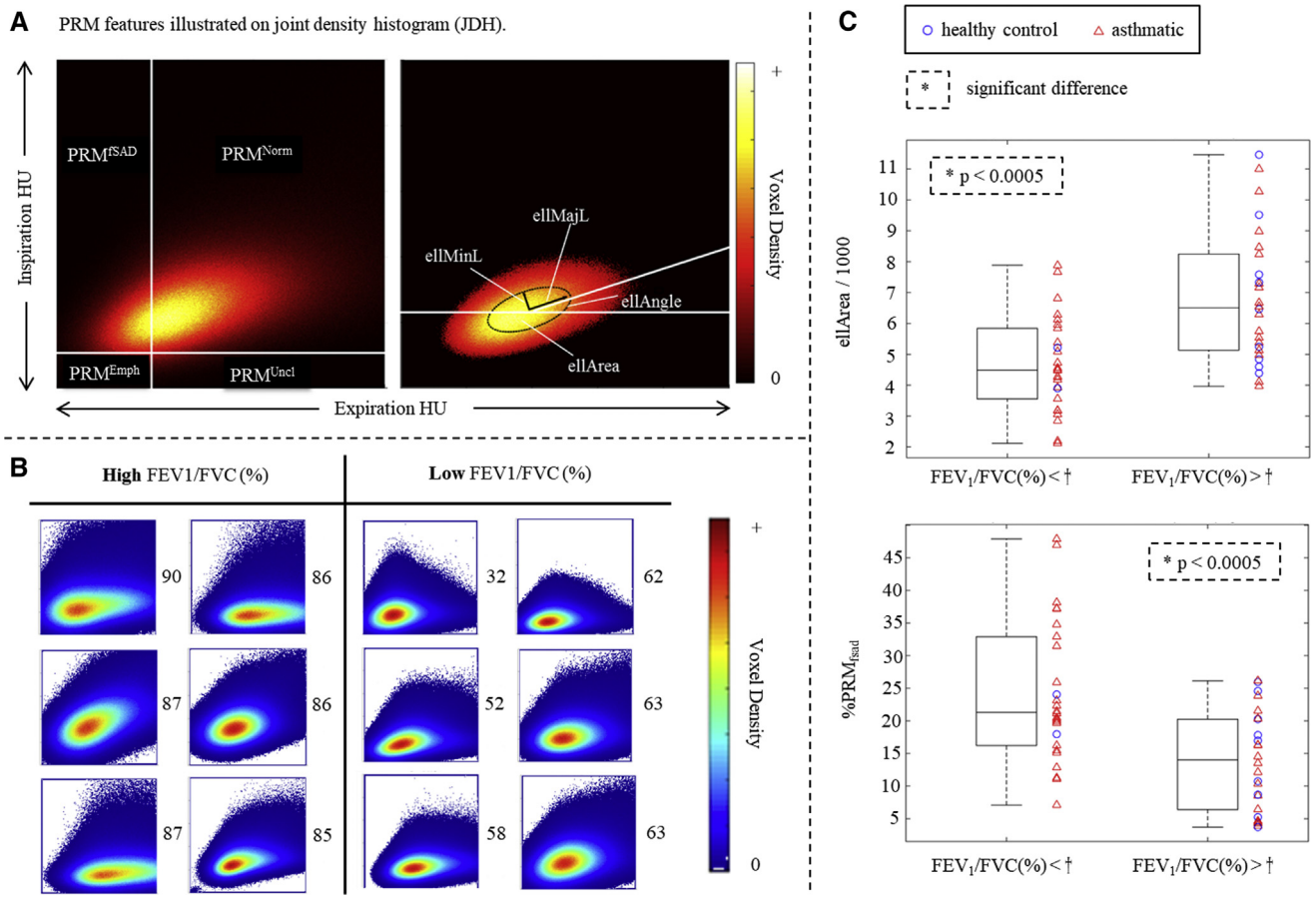

FIG 1. Global PRM mapping and spirometry. **A,** PRM features based on TLC and FRC HU joint density histogram *(JDH)*. PRM voxel classification *(left)* was defined by lines of expiration (HU = −856) and inspiration (HU = −950) used for defining PRM^{fSAD} and PRM ellipse geometry. **B,** JDH visualization of FEV_1/FVC ratio (as a percentage) in extreme cases, demonstrating compact and left-shifted ellipses in patients with airflow obstruction. **C,** Box plot illustrating that patients with spirometric airflow obstruction have smaller PRM ellipse areas and significantly more fSAD on CT imaging ($\%PRM^{fSAD}$); groups were formed about median FEV_1/FVC ratios (percentages).

Body plethysmography was performed with a constant-volume plethysmograph, according to the ATS/ERS recommendation.[30] A minimum of 3 acceptable tests were performed, and the test ended when the repeatability criterion was achieved (FRC within 10% between the highest and lowest values). Carbon monoxide uptake in the lung was determined by using the single-breath method, according to standard guidelines.[31] Alveolar volume and the carbon monoxide transfer coefficient were calculated.

CT imaging and image analysis

Volumetric whole-lung scans were obtained after administration of 400 μg of inhaled salbutamol at FRC and TLC in patients lying supine. CT images were quantified by using a panel of imaging biomarkers (see Table E1 in this article's Online Repository at www.jacionline.org).

PRM was performed automatically by using Imbio's Lung Density Analysis (LDA) software application (Imbio, Minneapolis, Minn) for all CT data, with registrations performed from TLC to FRC on segmented voxel sets, excluding the major airways (up to 3-4 generations from the trachea). Details on PRM analysis have been reported previously.[19-22] Relative lung volumes of normal parenchyma (PRM^{Norm}), patients with fSAD (PRM^{fSAD}), patients with emphysema (PRM^{Emph}), and unclassified parenchyma (PRM^{Uncl}) were calculated by normalizing the sum of all like-classed voxels by total lung volume. Additionally, features of the PRM joint density histogram (ellipse area, minor axis, major axis, and angle to horizontal) were derived in MATLAB 2015a (MATLAB Release 2015a; MathWorks, Natick, Mass; Fig 1, *A*).

A novel algorithm for evaluating regional density change gradients in a given direction, termed stratified axial analysis (SAA), was developed from per-voxel TLC to FRC density change (ΔHU; see Figs E1 and E2, *A*, in this article's Online Repository at www.jacionline.org). This allowed us to investigate how ventilation, approximated by ΔHU, varied with respect to axes of interest, particularly anterior-posterior (approximately parallel to gravity) and inferior-superior (approximately perpendicular to gravity; Fig 2, *C* and *D*). Straight-line fitting by using the ordinary least-squares criterion was applied to produce $std(\Delta HU)^{AP}$, $\overline{\Delta HU}^{AP}$, $std(\Delta HU)^{IS}$, and $\overline{\Delta HU}^{IS}$ as the gradients of fitted lines to SAA-derived intervals (see Fig E1), where *AP* and *IS* refer to the axis used (anterior-to-posterior and inferior-to-superior, respectively), *std* refers to SD, and $\bar{x}$ refers to the arithmetic mean of *x*. $\overline{\Delta HU}^{IS*}$ was calculated as the mean of $\overline{\Delta HU}$ values across every decile, equivalent to the scaled (1:9) difference of extreme interval averages in the inferior-superior direction. Additional markers classifying lung size asymmetry were also derived by using custom scripts in MATLAB (see Fig E2, *B*).

Computational simulations of regionalized bronchoconstriction

A detailed outline of the computational models is provided in the Methods section in this article's Online Repository at www.jacionline.org. Briefly, a

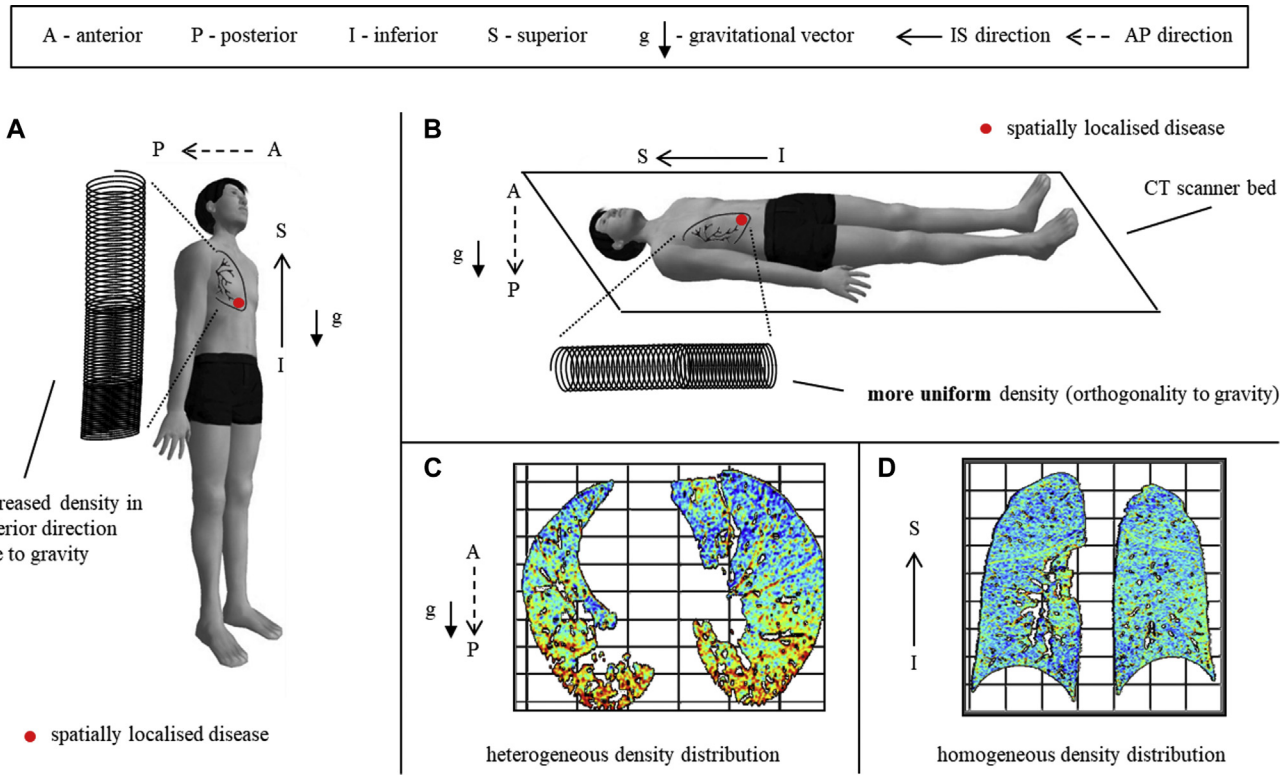

FIG 2. **A** and **B,** Overview of the slinky effect in the lungs in standing and supine postures demonstrating distribution of lung density as a consequence of gravity. **C,** It can be seen that in the supine posture the inferior-superior lung density profile will be largely independent of gravity (transverse cross-section of expiratory HU voxels), with expected largest volume of ventilation in the lower lobes caused by the lower lobe having the largest proportionate lung volume. **D,** In contrast, the anterior-posterior lung density profile will be predominantly influenced by gravity (coronal cross-section of expiratory HU voxels), such that posterior ventilation will be proportionately lower than anterior ventilation. ΔHU gradients in these 2 axes were used to understand the determinants of clinical VH measurements derived from IOS and MBW.

computational model of airway impedance was designed based on previous models in the literature to provide simulations of IOS-derived R5-R20. In short, a 1-dimensional wave equation was used to estimate the impedance of each branch,[32] with total impedance being calculated through summation of parallel and series contributions.[33] Each terminal bronchiole was subtended by using a constant-phase viscoelastic model parameterized by using data from the literature.[34] Models were adjusted for potential confounding by upper airway shunting.[35,36]

Simulations of total lung resistance over the frequency range (1-25 Hz) were performed on the healthy conducting airway tree created through a combination of CT segmentation (to an average generation of 6) and algorithmic generation (to an average generation of 16), as previously reported.[37] For each simulation, constrictions were applied to either the lowest or highest 25% of small airways (≤2 mm in diameter) relative to the supine or orthostatic position to simulate the effects of gravitationally dependent airways. Constriction rates (percentage reduction in airway denoted as *c*) were drawn uniformly from the range (0% to 70%) and applied homogeneously by using the same c value for all airways or heterogeneously by drawing each constriction from the normal distribution with mean c value and SD of 0.2c. For each simulation, the output R5-R20 value was calculated.

Statistical analysis

Statistical analyses were performed in MATLAB 2015a. Kolmogorov-Smirnov tests were applied to check the likelihood of a normal distribution. Binary group comparisons were performed by using a 2-sample *t* test (parametric data) and Mann-Whitney *U* test (nonparametric data); for multiple-group comparisons, 1-way ANOVA (parametric data) and the Kruskal-Wallis test (nonparametric data) were used. Multiple-comparison procedures were performed with the Tukey honest significant difference criterion. Subgroups were determined based on GINA treatment steps and according to mean S_{acin} and R5-R20 values. Sixteen subjects (roughly one third of the total population) at each end of R5-R20 and S_{acin} distributions were used in tertile polar analysis at SAA inferior-superior deciles, where statistical significance was determined by using the 2-sided Wilcoxon rank sum test.

The average Pearson correlation coefficient ($\bar{r}$) is reported for simple linear correlations. CT biomarker sets were defined by using Kaiser-Rule–determined principal component analysis and used for linear regression analyses to evaluate correlation with clinical traits and physiology. Linear discriminant analysis (LDA) was applied to determine class separation of the VH markers S_{acin} and R5-R20 by using combinations of CT imaging features, clinical features, and spirometry. Negative binomial regression was used to evaluate the relationship between exacerbations and imaging biomarkers and Pearson correlations for association between asthma control/quality of life and imaging ventilation gradient biomarkers.

A *P* value of less than .05 was used to define statistically significant results in all tests.

RESULTS

Clinical characteristics of the population are outlined in Table I. Asthmatic patients were matched for age and sex to healthy volunteers. The asthmatic population had significantly greater eosinophilic airway inflammation and physiologic evidence of airway dysfunction and VH when compared with healthy volunteers.

TABLE I. Clinical characteristics of asthmatic patients and healthy subjects

	Healthy volunteers (n = 11)	Asthmatic patients			
		All (n = 41)	GINA 1 (n = 8)	GINA 2/3 (n = 20)	GINA 4/5 (n = 13)
Clinical					
Age (y)	54.1 ± 14.4	53.7 ± 12.6	53.0 ± 9.2	56.5 ± 12.8	49.7 ± 13.7
Sex (male/female)	6/5	18/23	3/5	10/10	5/8
BMI (kg/m^2)	28.8 ± 4.5	27.1 ± 4.9	25.2 ± 4.4	26.3 ± 4.6	29.4 ± 5.3
Atopic (yes/no)	3/8‡§	30/11	6/2†	16/4†	8/5
Smoking (pack years)	4.2 ± 7.8	7.3 ± 17.0	3.0 ± 4.9	5.0 ± 8.1	13.4 ± 27.9
No. of exacerbations (past 12 mo)	—	1.4 ± 2.1	0.5 ± 0.8	1.1 ± 2.3	2.2 ± 2.1
ACQ-6 score	—	1.27 ± 1.04	0.94 ± 0.85	1.22 ± 0.85	1.56 ± 1.35
AQLQ score	—	5.37 ± 1.11	5.94 ± 0.90	5.28 ± 1.21	5.15 ± 1.00
Asthma duration (y)	—	17.6 ± 16.7	13.3 ± 9.5	18.9 ± 18.3	18.2 ± 18.2
Beclomethasone dipropionate equivalent ICS dose (μg/24 h)	—	820 ± 698	100 ± 282§‖	650 ± 371‡‖	1523 ± 656‡§
Physiology					
Post-BD FEV_1 (L)	3.7 ± 1.0*‡§	2.7 ± 0.80†	2.5 ± 0.68†	2.8 ± 0.85†	2.7 ± 0.81
Post-BD FEV_1 (%)	116 ± 19*	97.2 ± 20†	99.5 ± 20.8	97.7 ± 15.5	95.1 ± 26.3
Post-BD FEV_1/FVC (%)	80 ± 3.2	74 ± 11	76 ± 11	76 ± 7.6	72 ± 15
Bronchodilator response (% FEV_1)	3.62 ± 3.38*	12.88 ± 16.33†	8.79 ± 8.19	11.31 ± 13.52	17.80 ± 22.77
RV/TLC (%)	32.10 ± 7.71*	38.83 ± 8.68†	38.36 ± 8.41	40.43 ± 9.65	36.48 ± 7.13
KCO (% predicted)	96.15 ± 12.69*	104.65 ± 15.78†	101.13 ± 14.68	108.30 ± 15.53	100.92 ± 16.77
MBW					
LCI	7.32 ± 1.01	7.80 ± 1.28	7.51 ± 1.93	7.75 ± 1.01	8.05 ± 1.24
S_{acin}	0.131 ± 0.052*	0.207 ± 0.116†	0.193 ± 0.185	0.203 ± 0.097	0.220 ± 0.097
S_{cond}	0.037 ± 0.034	0.035 ± 0.024	0.034 ± 0.026	0.039 ± 0.026	0.028 ± 0.018
IOS					
R5-R20 (Kpa · s · L^{-1})	0.033 ± 0.029	0.061 ± 0.058	0.055 ± 0.035	0.053 ± 0.042	0.077 ± 0.085
AX (Kpa/L)	0.291 ± 0.219*	0.639 ± 0.752†	0.555 ± 0.423	0.457 ± 0.298	0.971 ± 1.209
Induced sputum					
Eosinophils (%)	0.46 ± 0.30*§	10.14 ± 28.17†	#	12.94 ± 35.70†	6.17 ± 6.76
Neutrophils (%)	46.32 ± 15.68	59.73 ± 24.47	37.13 ± 15.55	61.72 ± 27.02	63.96 ± 19.12

Data are expressed as means ± SDs. Attribute normality was tested by using the 1-sample Kolmogorov-Smirnov test over all subjects. Binary group comparisons (healthy subjects vs all asthmatic patients) were performed by using 2-sample *t* tests for parametric variables and Mann-Whitney *U* tests for nonparametric variables. Nonintersecting group comparisons were performed by using 1-way ANOVA for parametric variables and the Kruskal-Wallis test for nonparametric variables. Multiple-comparison procedures were performed with the Tukey honest significant difference criterion.

ACQ-6, 6-Item Juniper Asthma Control Questionnaire; *AQLQ*, standard 32-question Juniper Asthma Quality of Life Questionnaire; *AX*, area of reactance; *BD*, bronchodilator; *BMI*, body mass index; *ICS*, inhaled corticosteroid; *KCO*, carbon monoxide transfer coefficient; *LCI*, Lung Clearance Index; S_{cond}, conductive zone VH; *RV*, residual volume.

Groups with significant separation ($P < .05$) are indicated by the following superscripts:

*All asthmatic patients.

†Healthy control subjects.

‡GINA 1.

§GINA 2/3.

‖GINA 4/5, respectively.

There were no significant differences in values of the VH markers R5-R20 and S_{acin} across GINA treatment intensity groups. Of the 3 of 41 asthmatic patients with a smoking history of more than 15 pack years, all had a PRM emphysema (PRM^{Emph}) score that was less than the mean + 1.96 SD (5% PRM^{Emph}) in a healthy age-matched population of 98 subjects[38] and preserved carbon monoxide transfer coefficient percent predicted values (Table I). The 3 patients all had evidence of asthma objectively (1 had 78% FEV_1 reversibility, 1 had a PC_{20} methacholine value of 2 mg/mL, and 1 had 49% FEV_1 reversibility). Furthermore, of these 3 patients, only 2 demonstrated a postbronchodilator FEV_1/FVC ratio of less than the lower limit of normal (63% of predicted value in both patients, respectively, with a postbronchodilator FEV_1 percentage of 72% and 57%, respectively).

Imaging biomarkers of global lung VH are not associated with values of the small-airway VH markers R5-R20 and S_{acin}

Table E1 outlines the formal definition of all of the CT scan–derived imaging biomarkers. Table E2 in this article's Online Repository at www.jacionline.org presents comparisons of the global and regional imaging biomarkers, comparing asthmatic and healthy cases across the spectrum of GINA treatment intensity.

Asthmatic patients demonstrated significantly smaller PRM ellipse major diameters and smaller ellipse angles and had narrower distributions (SDs) of voxel HU change from FRC-TLC ($P < .05$) when compared with control subjects, which is indicative of less overall VH.

TABLE II. CT imaging biomarkers and VH-based stratification

	S_{acin}		R5-R20	
	Low (n = 29)	**High (n = 23)**	**Low (n = 32)**	**High (n = 20)**
Clinical				
Asthmatic patients/healthy subjects	20/9	21/2	24/8	17/3
PRM				
$\%PRM^{Norm}$	0.74 ± 0.11	0.71 ± 0.14	0.72 ± 0.14	0.73 ± 0.09
$\%PRM^{fSAD}$	0.19 ± 0.10	0.19 ± 0.12	0.19 ± 0.12	0.18 ± 0.08
$\%PRM^{Emph}$	0.024 ± 0.018	0.038 ± 0.037	0.032 ± 0.033	0.028 ± 0.021
$\%PRM^{Uncl}$	0.046 ± 0.036	0.063 ± 0.030	0.053 ± 0.038	0.055 ± 0.028
PRM ellipse properties				
ellMajL	126.2 ± 30.0	130.2 ± 28.9	122.0 ± 28.3	137.5 ± 29.0
ellMinL†	55.1 ± 9.4	56.5 ± 11.8	**52.1 ± 9.1**	**61.4 ± 10.0**
ellArea†	5590 ± 2067	5922 ± 2251	**5092 ± 1763**	**6769 ± 2312**
ellAngle	0.21 ± 0.13	0.16 ± 0.09	0.19 ± 0.11	0.20 ± 0.11
Ventilation gradient (ΔHU)				
$std(\Delta HU)^{AP}$	0.070 ± 0.078	0.059 ± 0.057	0.055 ± 0.068	0.080 ± 0.070
$\overline{\Delta HU}^{AP}$†	0.473 ± 0.207	0.450 ± 0.234	**0.512 ± 0.226**	**0.386 ± 0.183**
$std(\Delta HU)^{IS}$*	**−0.077 ± 0.043**	**−0.046 ± 0.035**	−0.064 ± 0.040	−0.062 ± 0.047
$\overline{\Delta HU}^{IS}$*†	**−0.043 ± 0.112**	**0.021 ± 0.099**	**−0.051 ± 0.100**	**0.044 ± 0.102**
$\overline{\Delta HU}^{IS*}$*†	**−2.033 ± 4.372**	**0.489 ± 3.936**	**−2.282 ± 4.018**	**1.267 ± 3.987**

Data are expressed as means ± SDs. Attribute normality was tested by using the 1-sample Kolmogorov-Smirnov test over all subjects. Binary group (ie, low S_{acin} vs high S_{acin} and low R5-R20 vs high R5-R20) comparisons were performed by using 2-sample *t* tests for parametric variables and Mann-Whitney *U* tests for nonparametric variables.
ellAngle, Ellipse angle to horizontal (radians); *ellArea*, ellipse area; *ellMajL*, ellipse major axis length; *ellMinL*, ellipse minor axis length.
Groups with significant separation ($P < .05$): *S_{acin} and †R5-R20; values formatted in boldface.

Asthmatic patients did not differ from control subjects with respect to standard PRM markers (PRM^{Norm}, PRM^{fSAD}, and PRM^{Emph}; see Table E2). In contrast, patients who demonstrated FEV_1/FVC ratios (percentages) of less than the median population value (primarily asthmatic patients) had higher levels of PRM^{fSAD} and smaller PRM global ellipse areas (suggestive of less global heterogeneity) when compared with patients with FEV_1/FVC ratios (percentages) of greater than or equal to the median value ($P < .05$; Fig 1, *B* and *C*). These observations were not replicated with the small-airway indices of VH R5-R20 and S_{acin} (see Fig E3 in this article's Online Repository at www.jacionline.org) and indicate that global PRM indices in the lung track with spirometry-defined airflow obstruction in contrast to small-airway physiologic indices.

Imaging biomarkers of regional VH are major determinants of the small-airway VH markers R5-R20 and S_{acin}

The population was split into low/high subgroups (low ≤ mean and high > mean) according to absolute S_{acin} and R5-R20 values to evaluate the relationship between regional imaging measures and small-airways physiology. Table II and Tables E3 (clinical features) and E4 (imaging markers) in this article's Online Repository at www.jacionline.org summarize clinical and imaging features according to this stratification. Healthy cases predominated in the groups with low S_{acin} (9/11) and low R5-R20 (8/11) values and asthmatic patients in the groups with high values.

Regional analysis identified that the gradient markers evaluating inferior-superior axis FRC-TLC deformation ($\overline{\Delta HU}^{IS}$ and $\overline{\Delta HU}^{IS*}$) slopes were the only markers that differed significantly in patients in the upper tertile of S_{acin} and R5-R20 values when compared with the lower tertile ($P < .05$, Table II). Specifically for patients with both high S_{acin} and R5-R20 values, the ventilation gradient was reversed in the inferior-superior axis ($\overline{\Delta HU}^{IS}$ and $\overline{\Delta HU}^{IS*}$), such that ventilation was significantly reduced at the base of the lung. This is further exemplified in Fig 3, which presents ventilation gradient maps from the base to the apex of the lung comparing cases within the upper and lower tertiles of R5-R20 and S_{acin}, respectively, and 2 exemplar subjects with and without ventilation gradient reversal. A similar but markedly less pronounced gradient change could be seen in the posterior regions of the lower lobes (anterior-posterior axis [$\overline{\Delta HU}^{AP}$]) when comparing patients with high and low clinical levels of VH (R5-R20 and S_{acin}), demonstrating reduced posterior ventilation in the lower lobes (see Fig E4 in this article's Online Repository at www.jacionline.org).

Further examination (Fig 4) of the distribution of ΔHU and regional PRM^{fSAD} in cases with high and low $\overline{\Delta HU}^{IS*}$ values identified that patients with high $\overline{\Delta HU}^{IS*}$ (ventilation gradient reversal) values appeared to have focused regionalization of lung disease (particularly but not exclusively in the lower lobes). In contrast, patients with a low $\overline{\Delta HU}^{IS*}$ value had more homogeneous distributions of both ΔHU and PRM^{FSAD}.

Fifteen of 16 cases with high $\overline{\Delta HU}^{IS*}$ values had abnormal regional ventilation in contrast to 5 of 16 cases with low $\overline{\Delta HU}^{IS*}$ values. Regionalization of disease in all of these cases was in the lower lobes, generally focused at lung bases (see arrows). A χ^2 analysis of the proportions of cases with abnormal regionalization in each group demonstrated a *P* value of less than .0001. ΔHU and PRM classifications correlated imperfectly (Fig 4); however, lower ΔHU voxels were consistently associated with PRM^{fSAD} (see Fig E5 in this article's Online Repository at www.jacionline.org).

Imaging gradient biomarkers and clinical disease

We examined the relationship between the imaging gradient biomarkers and clinical disease expression (Table II, see Tables E5-E7 in this article's Online Repository at www.jacionline.org).

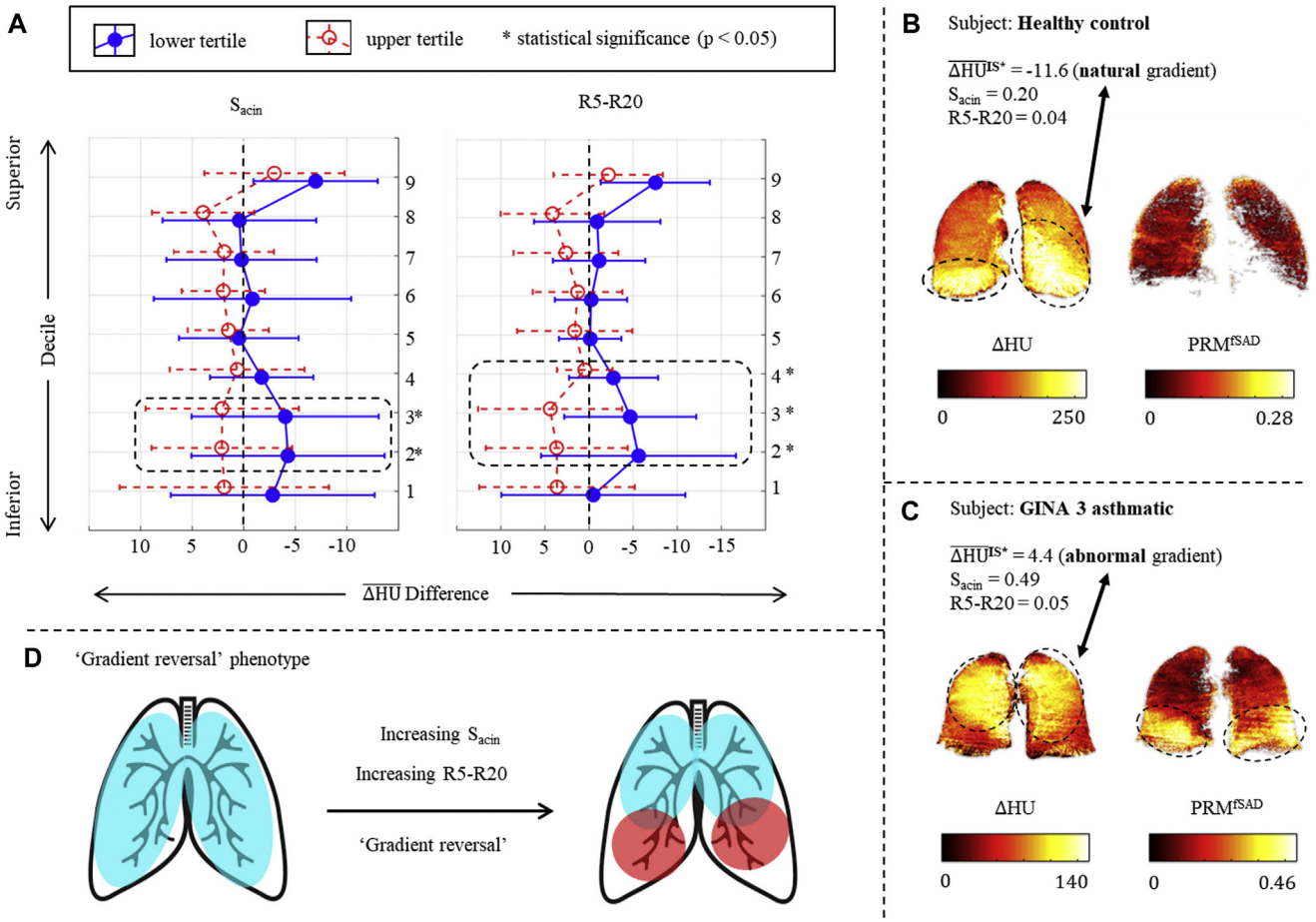

FIG 3. Inferior-superior ΔHU gradient analysis in patients with high/low S_{acin} and R5-R20 values. **A,** Decile-wise comparison of ΔHU mean differences in the inferior-to-superior direction of groups formed from the lower and upper tertiles of S_{acin} and R5-R20 distributions, specifically the lowest and highest 16 subjects with respect to these 2 markers. The inferior regions show significant differences when comparing lower and upper tertiles for both S_{acin} and R5-R20 values. **B,** Joint density histogram of voxel mean ΔHU and PRM^{fSAD} percentages when projected onto the coronal plane in subjects showing the typical (healthy) ventilation (surrogated by ΔHU) pattern and homogenous PRM^{fSAD}. **C,** As in Fig 3, *B*, but in a subject with an abnormal ventilation pattern and basally focused PRM^{fSAD}. Color bars labeled with minimums and maximums of mean values. **D,** Concept of the inferior-superior gradient reversal phenotype is summarized in a simple visual schematic.

We found that anterior posterior gradient imaging biomarker $std(\Delta HU)^{AP}$ correlated significantly with both 6-item Juniper Asthma Control Questionnaire ($r = 0.33$, $P = .039$) and standard 32-question Juniper Asthma Quality of Life Questionnaire ($r = -0.34$, $P = .02$) scores. We also found a significant association for the inferior-superior gradient imaging biomarker ($\overline{\Delta HU}^{IS*}$) and asthma-related quality of life ($r = -0.39$, $P < .01$) but not asthma control. None of the gradient biomarkers were associated with exacerbation frequency.

Discrimination of S_{acin} and R5-R20 with imaging markers of density change (ΔHU) gradients and lung size asymmetry

Fig 5 and Tables E8 and E9 in this article's Online Repository at www.jacionline.org present the results of LDA, which was used to identify the relative contribution of spatial CT-derived VH biomarkers, potential clinical contributors/confounders, and spirometry to the physiologic VH indices S_{acin} and R5-R20. LDA demonstrated that the CT markers of ΔHU in the inferior-superior and anterior-posterior axes, as well as right to left lung size asymmetry, provided the greatest overall discriminatory value of small-airways physiologic indices, confirming that these metrics contained most of the information content of the clinical small-airways physiologic indices.

Computational modeling validation of CT imaging PRM gradients

Computational modeling of regional bronchoconstriction in small-airway patient-specific conducting airway models (Fig 6) identified that increasing constriction of the small airways (≤2 mm diameter), which would be most influenced by gravity in the supine posture (lower lobe and posterior), promoted profound increases in R5-R20 values that were not seen with orthostatic simulations (ie, constriction of small airways that would be most influenced by gravity in the orthostatic posture). Furthermore, similar regional constriction in the upper lobes did not

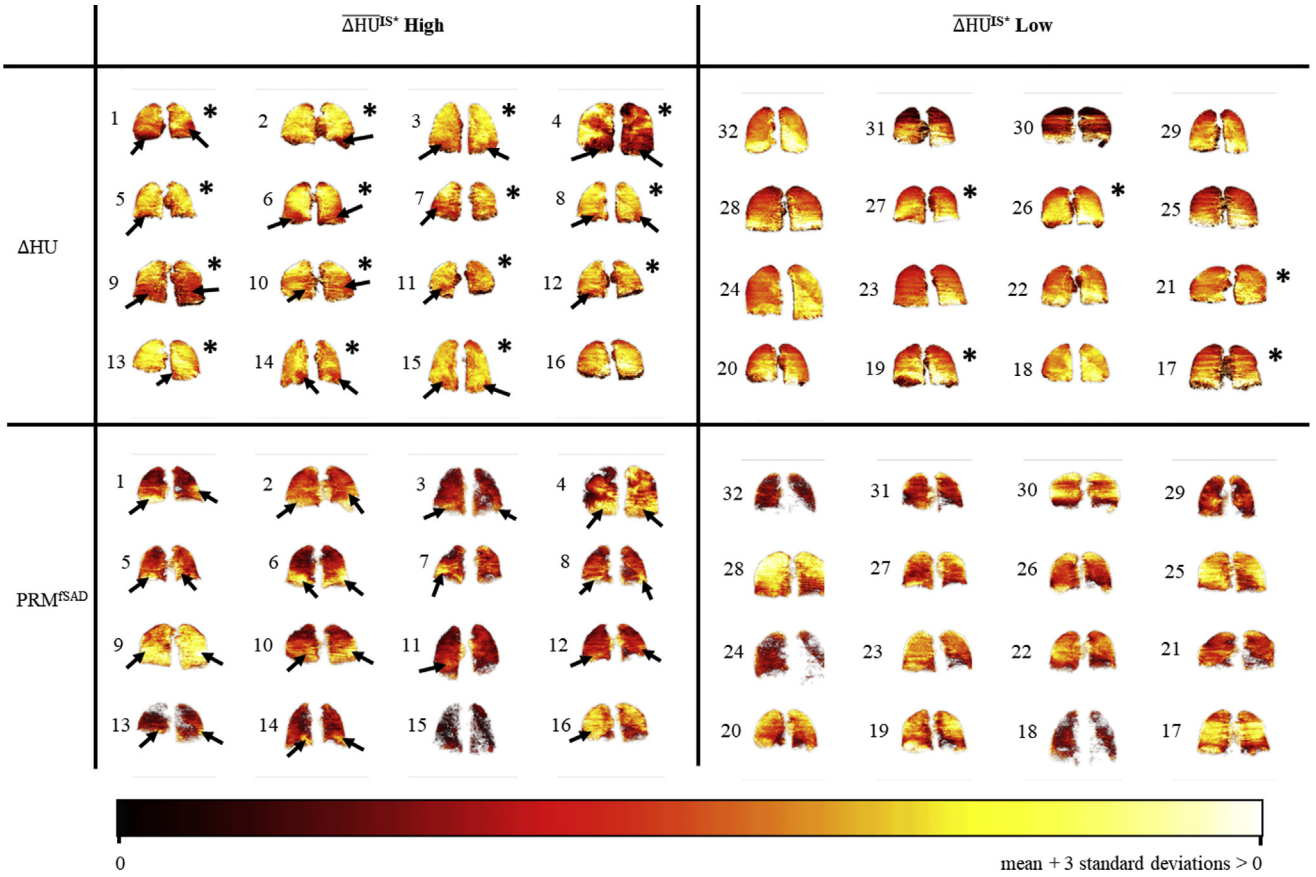

FIG 4. Coronal section heat maps of ΔHU and PRM^{fSAD} values in cases with low $\overline{\Delta HU}^{IS*}$ (no gradient reversal) and high $\overline{\Delta HU}^{IS*}$ (basal gradient reversal) tertiles of total population (n = 52). Images labeled with an ID number assigned with respect to decreasing $\overline{\Delta HU}^{IS*}$ values (eg, 1 = greatest $\overline{\Delta HU}^{IS*}$ [greatest level of inferior/lower zone gradient reversal] and 32 = smallest $\overline{\Delta HU}^{IS*}$ [lowest level of basal gradient reversal]. Nonasthmatic subjects *(H)* and asthmatic patients *(G)* with GINA levels are shown. It can be seen that patients with high $\overline{\Delta HU}^{IS*}$ values more often than not have inferior gradient reversal but also exhibit ΔHU and PRM^{fSAD} heterogeneity. In contrast, patients with a low $\overline{\Delta HU}^{IS*}$ value appear to have more homogeneous distributions of ΔHU and PRM^{fSAD} or upper lobe regionalization of low ΔHU, as would be expected in the supine posture. Color bar ranges were determined per subject based on feature (ΔHU or PRM^{fSAD}) mean and variance, as indicated. *Arrows* highlight specific disease regionalization in subjects with abnormal $\overline{\Delta HU}^{IS*}$ values. *Asterisks* indicate subjects selected for χ^2 tests of proportions, having abnormal regionalization of ventilation.

promote the same difference on R5-R20 values when considering orthostatic and supine postures. Therefore the computational models provided further insight into associations between the lower-lobe regional focus of disease and R5-R20 response seen in the clinical imaging study (Figs 3 and 4).

DISCUSSION

We performed the first quantitative functional CT imaging study to understand the spatial determinant of the small-airway VH markers R5-R20 and S_{acin} in adult asthmatic patients and healthy volunteers. Furthermore, we have coupled CT imaging with computational simulation of small-airway physiology to understand the effect of the disease's regional pattern on abnormal physiologic indices of VH.

Using a panel of imaging biomarkers (Table E1) derived from inspiratory and expiratory CT scans, we have identified that gradients in ΔHU from the base to apex of the lung are key determinants of both physiologic measurements. Notably, there is a reversal of the normal ventilation gradient in this axis, such that ΔHU is reduced at the base of the lung in patients with asthma and indeed occasionally in healthy volunteers with abnormal S_{acin} and R5-R20 values. In addition, we have identified that other mechanisms, including anterior-posterior ΔHU gradient decrease and other nonspecific regionalization of ΔHU might underpin abnormal R5-R20 and S_{acin} indices in adult asthmatic patients. We found broadly similar but not identical results with the widely reported markers of small-airways disease PRM^{fSAD} values. Computational small-airway tree models were then used to confirm the effect of gravitationally dependent lower-lobe disease regional focus on the IOS marker R5-R20 and matched our observation closely.

Previous studies have examined the difference in VH between asthmatic patients and healthy subjects by using hyperpolarized helium-3 MRI,[3] and another linked hyperpolarized helium-3 MRI with computational models to examine airway constriction in asthmatic patients.[39] We are also aware of one study in patient with bronchiectasis that attempted to correlate the global burden

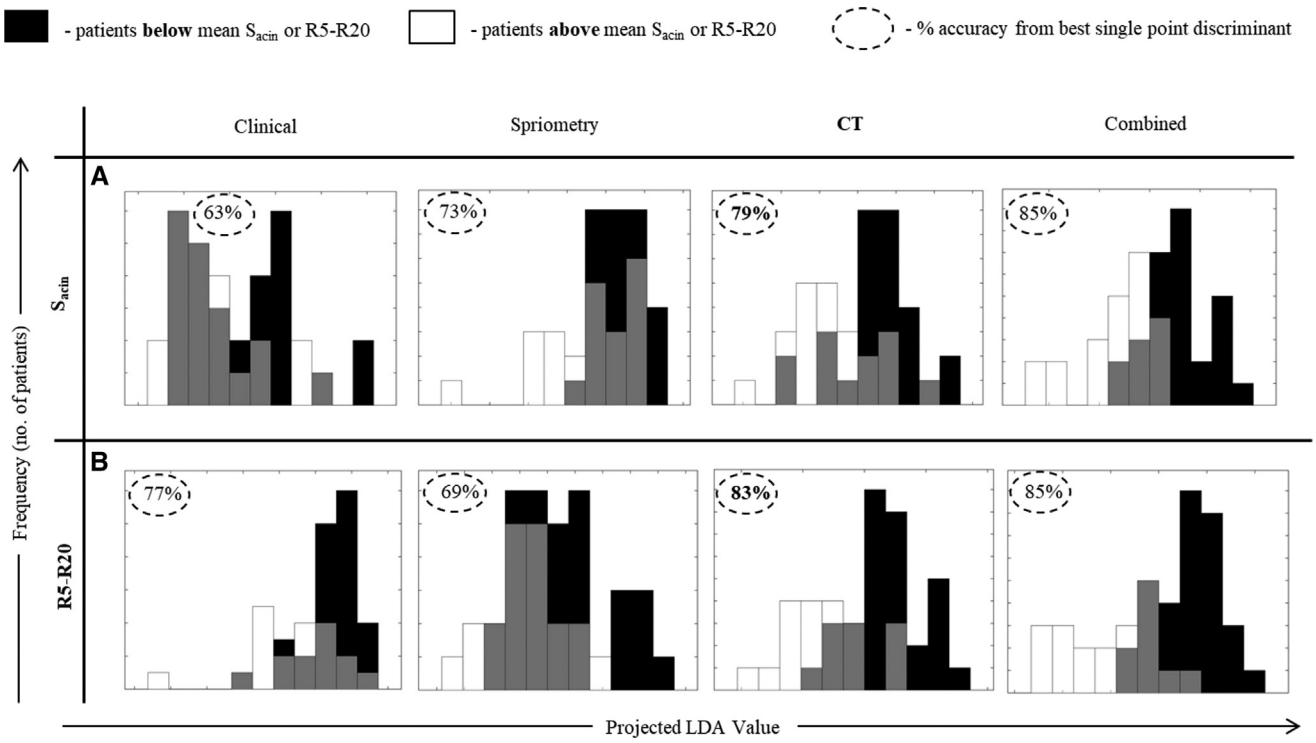

FIG 5. Histograms of LDA applied to the total population (n = 52) and showing the best linear separation of clinical VH, R5-R20, and S_{acin} values. Limited additional discrimination is added when considering potential clinical confounders of VH (eg, age, height, and weight), and spirometric results appear to be less sensitive at discriminating patients with normal and abnormal clinical VH than CT imaging.

of CT-determined disease with physiologic indices of VH.[40] This study used correlations and regressions to identify associations between MBW Lung Clearance Index scores (a global marker of VH) and CT scores of the extent of bronchiectasis.

Our study uses quantitative functional CT-derived indices and specifically sheds insight into the topographical origins of abnormal R5-R20 (IOS-derived) and S_{acin} (MBW-derived) VH markers. Furthermore, our observations, coupled with computer simulations (Figs 3, 4, and 6) suggest that regionalization rather than global disease burden might be key determinants of S_{acin} and R5-R20 in asthmatic patients.

Our results are clinically important for a number of reasons. Reduced basal ventilation in asthmatic patients can be associated with reduced effective deposition of inhaled drugs, which might be a factor in the poor asthma control reported in patients receiving inhaled corticosteroid/long-acting β-agonist combination therapies in European and other populations[41]; this hypothesis would require testing with future studies. Additionally, our findings are important because they are the first to use spatial and functional information derived from quantitative PRM-based CT imaging to shed insight into empiric lung physiologic measurements R5-R20 and S_{acin}, which are widely reported as small-airway dysfunction detection tools.

Interestingly, we found few differences in the PRM whole-lung averages for patients with fSAD, patients with emphysema, and healthy subjects (normally deforming lung voxels) in those with and without high levels of clinical VH derived from MBW and IOS. In contrast, average whole-lung PRM values were associated with airflow obstruction measured by using spirometry. The latter observations highlight both the importance of using the full information content of spatial imaging when trying to understand the topographical basis of VH indices and the fact that expiratory flow limitation in asthma is a maker of total burden of lung unit damage rather than the heterogeneity of damage.

A likely factor of the observed ventilation gradients in the lung is the "slinky" effect, which describes the compression of a slinky coil parallel to the gravitational field under normal gravitational conditions, isogravity, and hypergravity.[42] Because the dependent regions of the lung are compressed by the weight of the lung above them, they have lower end-expiratory volume, and the surrounding pleural pressure is more positive (in comparison with the apex); consequently, a given respiratory effort and change in pleural pressure will lead to a larger increase in volume.

Other factors responsible for ventilation and perfusion gradients are likely to include lung elastic recoil, nonlinear pressure-volume relationships, the influence of large vessels, and airway closure within dependent airways. These effects have been reported in imaging studies using both protocol MRI approaches[43] and, more recently, a CT imaging lung deformation study in patients with severe asthma.[19]

The finding of a reverse ΔHU gradient at the base of the lung in patients with abnormal S_{acin} and R5-R20 values and asthma can occur as a consequence of a number of factors in asthmatic patients. Specifically, basal airways can close at FRC in asthmatic patients, particularly when supine, and this can reduce the specific ventilation to the lung base; one study observed results to this effect in airway constriction because of methacholine challenge.[44] Additionally, the average BMI in our cohort was 30 kg/m^2; fat distribution in the abdomen and near the base of the lung can alter diaphragmatic and basal airway mechanics and promote airways

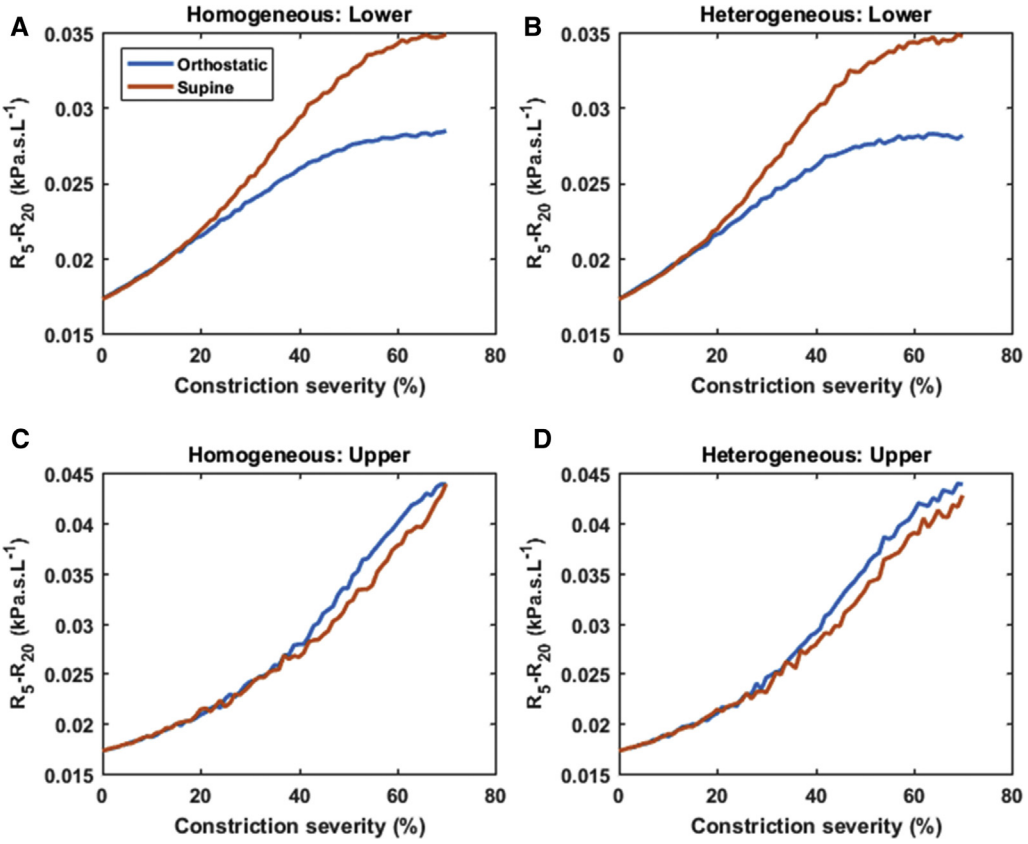

FIG 6. Comparison of R5-R20 values under varying regional small-airway constrictions applied to healthy lung structure. The R5-R20 response can be seen for homogeneous (**A** and **C**) and heterogeneous (**B** and **D**) constriction of the small airways. In each case constrictions were applied to the lowest or highest 25% of airways relative to the orthostatic or supine position. It can be seen that lower zone constriction and regionalization produce far greater increases in R5-R20 values than upper lobe constriction and regionalization, which is in keeping with the observations in Figs 3 and 4.

closure. Additionally, it is possible that there is preferential remodeling of the airways in the lung base in asthmatic patients. However, this would need to be confirmed by pathologic studies. Similar effects, including the effect of gravity, can promote the smaller anterior-posterior gradient decrease seen in patients with clinical VH. It is important to note that LDA identified that ventilation gradients were the best discriminant of R5-R20 independent of potential confounders, such as BMI, smoking, and age.

The current findings in this report add to our previous observations that have identified that both the degree and heterogeneity of small-airway obstruction promote abnormal R5-R20 values[45] and that S_{acin} can be driven by asymmetries in the lung at length scales that equate to the level of the alveolar duct.[9] Specifically, here we show that ventilation gradients in the lung are a major discriminant factor associated with both abnormal IOS-derived R5-R20 and MBW-derived S_{acin} values.

There are a number of limitations to our findings that warrant further evaluation. First, our study included asthmatic patients with a smoking pack year history of more than 15 pack years. Although these patients had no demonstrable imaging or physiologic evidence of emphysema, it is possible that smoking exposure rather than asthma *per se* was the driver of disease gradients in these patients. As a consequence, larger studies are required to evaluate the gradient biomarkers reported here across the spectrum of asthma severity and treatment intensity and in both smoking and nonsmoking asthmatic populations. The same limitation of sample size warrants further evaluation of the imaging biomarkers in populations of patients with severe asthma considering the association of the biomarkers with patient-related outcome measures in asthmatic patients. Such studies are underway and will be reported in due course.[46] Our imaging gradient biomarkers (derived through image registration of inspiratory and expiratory CT scans) are likely to be sensitive to both reconstruction kernel and lung volumes, as reported previously.[47] However, all of our CT scans were acquired at a single center with the same reconstruction kernel, and all patients were coached to expire to FRC for expiratory CT imaging before scanning. Nonetheless, it is possible that expiratory imaging near residual volume would accentuate the imaging findings observed here, and future studies are required to assess the effect of expiratory volume on the imaging biomarkers reported here.

In conclusion, we have shown, for the first time using functional and computational approaches derived from CT imaging, that small-airway VH captured by IOS-derived R5-R20 and MBW-derived S_{acin} values is associated with CT density gradient reversal at the lung base, which is likely to be a direct consequence of reduced specific ventilation and small-airways disease. The implications of these findings on clinical disease expression, inhaled drug deposition, and potential use in targeted

inhaled drug delivery systems should now be considered in larger imaging cohorts and interventional studies.

Clinical implications: Asthmatic patients with abnormal small-airways VH measurements demonstrated small-airways disease and reduced ventilation in the inferior regions of the lung, which might affect the effectiveness of inhaled therapies.

REFERENCES

1. Lui JK, Lutchen KR. The role of heterogeneity in asthma: a structure-to-function perspective. Clin Transl Med 2017;6:29.
2. Teague WG, Tustison NJ, Altes TA. Ventilation heterogeneity in asthma. J Asthma 2014;51:677-84.
3. Tzeng YS, Lutchen K, Albert M. The difference in ventilation heterogeneity between asthmatic and healthy subjects quantified using hyperpolarized 3He MRI. J Appl Physiol 2009;106:813-22.
4. Tahir BA, Van Holsbeke C, Ireland RH, Swift AJ, Horn FC, Marshall H, et al. Comparison of CT-based lobar ventilation with 3He MR imaging ventilation measurements. Radiology 2015;278:585-92.
5. Zha W, Kruger SJ, Johnson KM, Cadman RV, Bell LC, Liu F, et al. Pulmonary ventilation imaging in asthma and cystic fibrosis using oxygen-enhanced 3D radial ultrashort echo time MRI. J Magn Reson Imaging 2018;47:1287-97.
6. Venegas J, Winkler T, Harris RS. Lung physiology and aerosol deposition imaged with positron emission tomography. J Aerosol Med Pulm Drug Deliv 2013;26:1-8.
7. Farrow CE, Salome CM, Harris BE, Bailey DL, Berend N, King GG. Peripheral ventilation heterogeneity determines the extent of bronchoconstriction in asthma. J Appl Physiol 2017;123:1188-94.
8. Verbanck S, Paiva M. Gas mixing in the airways and airspaces. Compr Physiol 2011;1:809-34.
9. Gonem S, Hardy S, Buhl N, Hartley R, Soares M, Kay R, et al. Characterization of acinar airspace involvement in asthmatic patients by using inert gas washout and hyperpolarized 3helium magnetic resonance. J Allergy Clin Immunol 2016;137:417-25.
10. Galant SP, Komarow HD, Shin HW, Siddiqui S, Lipworth BJ. The case for impulse oscillometry in the management of asthma in children and adults. Ann Allergy Asthma Immunol 2017;118:664-71.
11. Oostveen E, MacLeod D, Lorino H, Farre R, Hantos Z, Desager K, et al. The forced oscillation technique in clinical practice: methodology, recommendations and future developments. Eur Respir J 2003;22:1026-41.
12. Robinson P, Latzin P, Verbanck S, Hall GL, Horsley A, Gappa M, et al. Consensus statement for inert gas washout measurement using multiple and single breath tests. Eur Respir J 2013;14:507-22.
13. Gonem S, Natarajan S, Desai D, Corkill S, Singapuri A, Bradding P, et al. Clinical significance of small airway obstruction markers in patients with asthma. Clin Exp Allergy 2014;44:499-507.
14. Farah CS, King GG, Brown NJ, Downie SR, Kermode JA, Hardaker KM, et al. The role of the small airways in the clinical expression of asthma in adults. J Allergy Clin Immunol 2012;129:381-7.
15. Thompson BR, Douglass JA, Ellis MJ, Kelly VJ, O'hehir RE, King GG, et al. Peripheral lung function in patients with stable and unstable asthma. J Allergy Clin Immunol 2013;131:1322-8.
16. Galvin I, Drummond GB, Nirmalan M. Distribution of blood flow and ventilation in the lung: gravity is not the only factor. Br J Anaesth 2007;98:420-8.
17. Gupta S, Hartley R, Khan UT, Singapuri A, Hargadon B, Monteiro W, et al. Quantitative computed tomography–derived clusters: redefining airway remodeling in asthmatic patients. J Allergy Clin Immunol 2014;133:729-38.
18. Shim SS, Schiebler ML, Evans MD, Jarjour N, Sorkness RL, Denlinger LC, et al. Lumen area change (Delta Lumen) between inspiratory and expiratory multidetector computed tomography as a measure of severe outcomes in asthmatic patients. J Allergy Clin Immunol 2018;142:1773-80.e9.
19. Choi S, Hoffman EA, Wenzel SE, Tawhai MH, Yin Y, Castro M, et al. Registration-based assessment of regional lung function via volumetric CT images of normal subjects vs. severe asthmatics. J Appl Physiol 2013;115:730-42.
20. Galbán CJ, Han MK, Boes JL, Chughtai KA, Meyer CR, Johnson TD, et al. Computed tomography–based biomarker provides unique signature for diagnosis of COPD phenotypes and disease progression. Nat Med 2012;18:1711.
21. Boes JL, Hoff BA, Bule M, Johnson TD, Rehemtulla A, Chamberlain R, et al. Parametric response mapping monitors temporal changes on lung CT scans in the subpopulations and intermediate outcome measures in COPD Study (SPIROMICS). Acad Radiol 2015;22:186-94.
22. Bhatt SP, Soler X, Wang X, Murray S, Anzueto AR, Beaty TH, et al. Association between functional small airway disease and FEV1 decline in chronic obstructive pulmonary disease. Am J Respir Crit Care Med 2016;194:178-84.
23. 2018 GINA report: global strategy for asthma management and prevention. Available at: https://ginasthma.org/2018-gina-report-global-strategy-for-asthma-management-and-prevention/. Accessed January 9, 2019.
24. Heaney LG, Brightling CE, Menzies-Gow A, Stevenson M, Niven RM. Refractory asthma in the UK: cross-sectional findings from a UK multicentre registry. Thorax 2010;65:787-94.
25. Juniper EF, Svensson K, Mörk AC, Ståhl E. Measurement properties and interpretation of three shortened versions of the asthma control questionnaire. Respir Med 2005;99:553-8.
26. Juniper EF, Buist AS, Cox FM, Ferrie PJ, King DR. Validation of a standardized version of the Asthma Quality of Life Questionnaire. Chest 1999;115:1265-70.
27. Reddel HK, Taylor DR, Bateman ED, Boulet LP, Boushey HA, Busse WW, et al. An official American Thoracic Society/European Respiratory Society statement: asthma control and exacerbations: standardizing endpoints for clinical asthma trials and clinical practice. Am J Respir Crit Care Med 2009;180:59-99.
28. Miller MR, Hankinson JA, Brusasco V, Burgos F, Casaburi R, Coates A, et al. Standardisation of spirometry. Eur Respir J 2005;26:319-38.
29. Dutrieue B, Vanholsbeeck F, Verbanck S, Paiva M. A human acinar structure for simulation of realistic alveolar plateau slopes. J Appl Physiol 2000;89:1859-67.
30. Wanger J, Clausen JL, Coates A, Pedersen OF, Brusasco V, Burgos F, et al. Standardisation of the measurement of lung volumes. Eur Respir J 2005;26:511-22.
31. MacIntyre N, Crapo R, Viegi G, Johnson DC, Van Der Grinten CP, Brusasco V, et al. Standardisation of the single-breath determination of carbon monoxide uptake in the lung. Eur Respir J 2005;26:720-35.
32. Benade AH. On the propagation of sound waves in a cylindrical conduit. J Acoust Soc Am 1968;44:616-23.
33. Kaczka DW, Massa CB, Simon BA. Reliability of estimating stochastic lung tissue heterogeneity from pulmonary impedance spectra: a forward-inverse modeling study. Ann Biomed Eng 2007;35:1722-38.
34. Lutchen KR, Gillis H. Relationship between heterogeneous changes in airway morphometry and lung resistance and elastance. J Appl Physiol 1997;83:1192-201.
35. Bhatawadekar SA, Leary D, Maksym GN. Modelling resistance and reactance with heterogeneous airway narrowing in mild to severe asthma. Can J Physiol Pharmacol 2015;93:207-14.
36. Cauberghs M, Van de Woestijne KP. Mechanical properties of the upper airway. J Appl Physiol 1983;55:335-42.
37. Bordas R, Lefevre C, Veeckmans B, Pitt-Francis J, Fetita C, Brightling CE, et al. Development and analysis of patient-based complete conducting airways models. PLOS One 2015;10:e0144105.
38. Boudewijn IM, Postma DS, Telenga ED, ten Hacken NH, Timens W, Oudkerk M, et al. Effects of ageing and smoking on pulmonary computed tomography scans using parametric response mapping. Eur Respir J 2015;46:1193-6.
39. Campana L, Kenyon J, Zhalehdoust-Sani S, Tzeng YS, Sun Y, Albert M, et al. Probing airway conditions governing ventilation defects in asthma via hyperpolarized MRI image functional modeling. J Appl Physiol 2009;106:1293-300.
40. Verbanck S, King GG, Zhou W, Miller A, Thamrin C, Schuermans D, et al. The quantitative link of lung clearance index to bronchial segments affected by bronchiectasis. Thorax 2018;73:82-4.
41. Partridge MR, van der Molen T, Myrseth SE, Busse WW. Attitudes and actions of asthma patients on regular maintenance therapy: the INSPIRE study. BMC Pulm Med 2006;6:13.
42. Hopkins SR, Henderson AC, Levin DL, Yamada K, Arai T, Buxton RB, et al. Vertical gradients in regional lung density and perfusion in the supine human lung: the Slinky effect. J Appl Physiol 2007;103:240-8.
43. Henderson AC, Sá RC, Theilmann RJ, Buxton RB, Prisk GK, Hopkins SR. The gravitational distribution of ventilation-perfusion ratio is more uniform in prone than supine posture in the normal human lung. J Appl Physiol 2013;115:313-24.
44. Soares M, Bordas R, Thorpe J, Timmerman B, Brightling C, Kay D, et al. Validation of impulse oscillometry R5-R20 as a small airways dysfunction detection tool in adult asthma. Eur Respir J 2016;48:OA4968.
45. Farrow CE, Salome CM, Harris BE, Bailey DL, Bailey E, Berend N, et al. Airway closure on imaging relates to airway hyper responsiveness and peripheral airway disease in asthma. J Appl Physiol 2012;113:958-66.
46. Postma DS, Brightling C, Fabbri L, van der Molen T, Nicolini G, Papi A, et al. Unmet needs for the assessment of small airways dysfunction in asthma: introduction to the ATLANTIS study. Eur Respir J 2015;45:1534-8.
47. Boes JL, Bule M, Hoff BA, Chamberlain R, Lynch DA, Stojanovska J, et al. The impact of sources of variability on parametric response mapping of lung CT scans. Tomography 2015;1:69-77.